

Structural Analysis of the Midshaft in an Isolated Femur from Koobi Fora, Kenya: Implications for Taxonomic Identity

MICHELE M. BLEUZE*

Department of Anthropology, California State University Los Angeles, 5151 State University Drive, Los Angeles, CA 90032, USA; mbleuze@calstatela.edu

*corresponding author: mbleuze@calstatela.edu

submitted: 18 August 2021; revised: 3 December 2021; second revision: 11 May 2022; accepted: 25 August 2022

ABSTRACT

Reconstructing hominin evolution is dependent on our capacity to securely and accurately allocate fossil hominin material to an appropriate taxon. While taxonomic assignments are traditionally based on craniodental morphology, structural analyses of unassociated hominin long bones have provided a means to deduce the taxonomic identity of isolated postcranial remains based on morphological comparisons with corresponding elements from craniodentally associated material. This study examines cross-sectional geometric properties in the mid-diaphyseal section in KNM-ER 1592, an unassociated femur from the KBS Member of the Koobi Fora Formation, Kenya. Hominin taxonomic diversity throughout this member has hindered attempts to taxonomically place KNM-ER 1592 based on stratigraphic location alone. The aim of this study is to infer the taxonomic identity of this femur based on morphometric comparisons with femora assigned to *Australopithecus*, *Paranthropus*, and *Homo*. Relationships between cortical area and total area, and differential bending rigidity along the anatomical planes of the midshaft femur were examined. Torsional and average bending strength in KNM-ER 1592 was compared to distributions in australopith, non-*habilis* early *Homo*, and *H. naledi* groups to further assess its midshaft structure in comparative context. The overall mid-diaphyseal femoral morphology in KNM-ER 1592 fits comfortably with patterns observed in non-*habilis* early *Homo* Pleistocene femora. KNM-ER 1592 shows an increase in cortical area for a given total area (i.e., relatively thick cortical bone) in the midshaft region like most pre-modern hominins. However, it displays a greater mediolateral relative to anteroposterior expanded mid-diaphyseal morphology characteristic of *H. erectus* and “*erectus*-like” femora, and its torsional and average bending strength further demonstrates its affinity with non-*habilis* early *Homo*. Based on the structural analyses of the mid-diaphyseal region, a tentative assignment of KNM-ER 1592 to genus *Homo* sp. indet. is supported. The alignment of KNM-ER 1592 with *Homo* is further supported when its overall cross-sectional size is also considered. Overlap among australopith and *Homo* samples at the smaller and intermediate size ranges is observed in both bivariate comparisons, but australopith and *Homo* samples do not overlap at the larger end of the size range where KNM-ER 1592 consistently falls with KNM-ER 803a and 1807. The former has been craniodentally aligned with *H. erectus* and the latter has been morphometrically aligned with *H. erectus* and “*erectus*-like” femora. Biomechanical analyses provide an avenue for which to test hypotheses about the taxonomic identity of isolated postcranial material based on morphological comparisons with material craniodentally attributed to a specific taxon.

INTRODUCTION

Our ability to reconstruct hominin evolution is dependent on our capacity to securely and accurately allocate fossil hominin material to an appropriate taxon, which is traditionally based on craniodental morphology. Although some postcranial elements unassociated with diagnostic craniodental material can be taxonomically placed, particularly when diagnostic morphological features are well-preserved and size-related shape variation is considered (Lague 2014; Susman et al. 2001), most isolated postcranial material remains taxonomically unidentified. There are practical and theoretical reasons that underlie the need

to identify isolated postcranial material at least to the genus level. Taxon-specific sample sizes can be maximized if the taxonomic identity of isolated elements can be reasonably estimated since these samples can then be included in analyses. Identifying the taxonomic affinity of isolated postcranial elements can broaden our knowledge about hominin postcranial diversity and expand our understanding of hominin evolution regarding morphological traits and morpho-functional complexes. Isolated material that can be taxonomically placed can serve as a resource for comparative purposes and to test hypotheses. For instance, Lague and colleagues (2019a) conducted morphometric

and comparative analyses of the elbow region in KNM-ER 47000, an unassociated partial upper limb skeleton that includes parts of the scapula, humerus, ulna, and hand, and found that the elbow, and by implication the upper limb, could reasonably be attributed to *Paranthropus boisei*. The taxonomic identification of KNM-ER 47000 as *P. boisei* has alleviated the dearth of postcranial material assigned to this taxon and has allowed researchers to test hypotheses about locomotor behavior and manual dexterity, and by extension the ability to make and use stone tools, in *P. boisei* (Lague et al. 2019b; Richmond et al. 2020).

The functional use of skeletal elements is recorded in bone structure (Currey 2003; Huijkes 1982; Martin and Burr 1989). Dynamic mechanical loading, particularly in weight-bearing bones, stimulates bone modeling and remodeling, which subsequently influences the cross-sectional geometry of a bone because bone tends to form and redistribute tissue in response to the loading environment (Lanyon and Rubin 1984; Woo et al. 1981). As a result, the cross-sectional geometry of a long bone can be examined to reconstruct mechanical loading patterns, yielding insight into function during life. Structural analyses of hominin long bones have primarily been used to reconstruct locomotor behavior across groups (e.g., Bleuze 2012; Friedl et al. 2019; Lovejoy et al. 2002; Marchi et al. 2019; Ohman et al. 1997; Ruff 2009; Ruff et al. 2016), but such analyses have also proven useful for inferring the taxonomic identity of isolated postcranial remains based on morphological comparisons with corresponding elements from craniodentally associated material (e.g., Cazenave et al. 2017; Lague 2015; Ruff et al. 2015). For instance, Grine and colleagues (1995) compared the external morphology and cross-sectional geometric properties in an isolated femur from Berg Aukas, Namibia, to a sample of australopiths, early and later *Homo*, early modern humans, and modern humans, and found that the Berg Aukas femur shared morphological affinities with femora of Middle Pleistocene archaic *H. sapiens* and Neandertals. A further assessment of its femoral diaphyseal cross-sectional geometry confirmed its affinity with Middle Pleistocene *Homo* femora (Trinkaus et al. 1999).

Previous studies have examined craniodentally unassociated femora from Koobi Fora, Kenya, within a comparative context for the purpose of taxonomic assessment. McHenry and Corruccini (1978) found KNM-ER 1472 and 1481a, two well preserved, virtually complete femora initially classified as *Homo* sp. indet. (Day et al. 1975; Leakey 1973a), to be morphometrically more similar to a sample of modern human femora than to a sample of australopith femora (SK 82, 97, and KNM-ER 1503) based on multivariate analyses of external dimensions across the femur. They concluded that the placement of KNM-ER 1472 and 1481a in genus *Homo* was justified (McHenry and Corruccini 1978). Based on comparisons of gross anatomy and multivariate analyses of internal (e.g., cortical index) and external (e.g., vertical femoral head diameter) osteometrics, Kennedy (1983a) concluded that KNM-ER 1481a could more specifically be attributed to *H. erectus*. Trinkaus (1984), however, argued that the traits Kennedy (1983a) used to align

KNM-ER 1481a with *H. erectus* are also generally found in archaic members of the genus *Homo*. He suggested that the stratigraphic association of KNM-ER 1481a with crania attributed to *H. habilis* (e.g., KNM-ER 1470, 1590, 3732) (now *H. rudolfensis*, Lieberman et al. 1996) and the similar degree of robusticity in KNM-ER 1481a and *H. habilis* postcranial material from Bed I Olduvai Gorge (e.g., OH 7, 8, 35) make it just as reasonable to consider KNM-ER 1481a as a representative of *H. habilis* (Trinkaus 1984: 139). Ruff (1995) found that structural properties in KNM-ER 1472, 1481a, and 3228 formed a morphological continuum with later *H. erectus* (e.g., OH 28) and were distinct from *H. habilis* (OH 62). He suggested the “*erectus*-like” KNM-ER 1472, 1481a, and 3228 possibly represented a lineage that evolved into *H. erectus* (Ruff 1995: 568).

This study examines cross-sectional geometric properties in the midshaft femur of KNM-ER 1592 to infer its taxonomic identity based on morphometric comparisons with femora attributed to *Australopithecus*, *Paranthropus*, and *Homo*. The unassociated partial femur dates to 1.85 million years ago (Ma) and was recovered from the KBS Member of the Koobi Fora Formation at East Turkana, Kenya (Feibel et al. 1989; Leakey and Walker 1985). Although there is an abundance of taxonomically unassigned isolated femora from Koobi Fora, KNM-ER 1592 is of particular interest for several reasons. The KBS Member is known for its hominin taxonomic richness including *Paranthropus* and multiple species of *Homo* (Bobe and Carvalho 2019), which has hindered attempts to taxonomically place KNM-ER 1592 based on stratigraphic location alone. Clarifying the taxonomic identity of KNM-ER 1592 will contribute to our understanding of hominin postcranial diversity and adaptations during a time when multiple hominin groups likely shared (and competed on) the landscape. Moreover, while both australopiths and *Homo* are represented in the KBS Member, the plethora of taxonomically uncertain material inhibits our ability to quantify taxonomic representation more accurately during this time and in this specific region of eastern Africa. In turn, this limits our capacity to address questions including generic population size and variation in generic establishment in a specific ecological niche. Inferences regarding the taxonomic identity of KNM-ER 1592 will contribute to reconstructions of temporospatial taxonomic representation (e.g., percent of generic or species abundance) in the KBS Member. Finally, a structural analysis of KNM-ER 1592 has not been conducted. Although australopith and early *Homo* femora may not always be distinguished based on external gross morphology, particularly when the proximal and distal ends of the bone are missing, some taxonomic distinctions based on structural differences have been observed in the mid-diaphyseal region (e.g., early *Homo* has a more weakly defined pilaster and a more expanded transverse diameter relative to sagittal diameter than *Australopithecus*) (Ruff 1995; Ruff et al. 2020; Ward et al. 2015). The KNM-ER 1592 femoral fragment preserves part of the diaphysis near the estimated midshaft making it suitable to test hypotheses about its taxonomic identity based on an assessment of its structural properties.

TABLE 1. FOSSIL SPECIMENS IN THIS STUDY.

Sample	Taxonomic attribution	Location	Geological age (Ma)	Ref. ^a
KNM-ER 736	<i>Homo</i> sp. indet.	Koobi Fora, Kenya	1.70	1, 2
KNM-ER 737	<i>H. erectus sensu lato</i>	Koobi Fora, Kenya	1.60	1, 3, 4
KNM-ER 803a	<i>H. erectus sensu lato</i>	Koobi Fora, Kenya	1.53	5
KNM-ER 1472	<i>Homo</i> sp. indet.	Koobi Fora, Kenya	1.89	6, 7
KNM-ER 1481a	<i>Homo</i> sp. indet.	Koobi Fora, Kenya	1.89	6, 7
KNM-ER 1807	<i>Homo</i> sp. indet.	Koobi Fora, Kenya	1.53	8
KNM-ER 1808m, n	<i>H. erectus sensu lato</i>	Koobi Fora, Kenya	1.70	9
KNM-ER 1592	<i>Australopithecus</i> or <i>Homo</i> sp. (?)	Koobi Fora, Kenya	1.85	10
OH 28	<i>H. erectus sensu lato</i>	Olduvai Gorge, Tanzania	0.7	11
OH 62	<i>H. habilis</i>	Olduvai Gorge, Tanzania	1.8	12
OH 80-12	<i>P. boisei</i>	Olduvai Gorge, Tanzania	1.34	13
AL 288-1	<i>Au. afarensis</i>	Hadar, Ethiopia	3.2	14
StW 99	<i>Au. africanus</i>	Sterkfontein, South Africa	2.0–2.6	15
StW 121	<i>Au. africanus</i>	Sterkfontein, South Africa	2.0–2.6	15
U.W. 101-003	<i>H. naledi</i>	Dinaledi Chamber, South Africa	0.236–0.335	16
U.W. 101-012	<i>H. naledi</i>	Dinaledi Chamber, South Africa	0.236–0.335	16
U.W. 101-268	<i>H. naledi</i>	Dinaledi Chamber, South Africa	0.236–0.335	16
Trinil II	<i>H. erectus sensu lato</i>	Trinil, Java	0.9–1.4	17
Trinil IV	<i>H. erectus sensu lato</i>	Trinil, Java	0.9–1.4	17
Trinil V	<i>H. erectus sensu lato</i>	Trinil, Java	0.9–1.4	17
Kresna 11	<i>H. erectus sensu lato</i>	Sangiran, Java	0.9–>1.5	18

^aReferences for descriptions of fossils and taxonomic assignments: 1. Leakey (1971); 2. Leakey et al. (1972); 3. Antón (2003); 4. Day and Leakey (1973); 5. Day and Leakey (1974); 6. Day et al. (1975); 7. Leakey (1973a); 8. Day et al. (1976); 9. Leakey and Walker (1985); 10. Leakey (1973b); 11. Day (1971); 12. Johanson et al. (1987); 13. Domínguez-Rodrigo et al. (2013); 14. Johanson et al. (1982); 15. DeSilva and Grabowski (2020); 16. Berger et al. (2015); 17. Day and Molleson (1973); 18. Grimaud-Hervé et al. (1994).

MATERIALS AND METHODS

KNM-ER 1592

The Koobi Fora Formation is in the Omo-Turkana Basin of northern Kenya along the northeastern shore of Lake Turkana. Pliocene and Pleistocene¹ deposits from the Koobi Fora Formation have yielded an abundance of fossil material including fossil hominins (Day 1986; Leakey and Leakey 1978). KNM-ER 1592 is the distal half of an isolated robust right femur (Leakey and Walker 1985). The fragment, which is approximately 200mm in length, was recovered from Area 12 in the lower KBS Member of the Koobi Fora Formation (Feibel et al. 1989; Leakey and Walker 1985). The KBS Member contains a sedimentary record from ~1.9–1.6 Ma (Lepre et al. 2007). *P. boisei* and at least three species of *Homo*—*H. habilis*, *H. rudolfensis*, and *H. erectus/ergaster* (or two species of *Homo* including *H. habilis sensu lato* and *H. erectus/ergaster*)—have been identified in the KBS Member (Bobe and Carvalho 2019; Feibel et al. 1989; Leakey and Leakey 1978). KNM-ER 1592 was initially provisionally attributed to *Australopithecus* based on external characteristics (Leakey 1973b). It was later observed to be similar in overall size and external morphology to KNM-ER 736 and 1808 (McHenry 1991). KNM-ER 736 is an isolated femur assigned to genus *Homo* based on morphological and structural comparisons with femora attributed to early *Homo*, and KNM-ER 1808 is an associated skeleton craniodentally assigned to *H. erectus* (Antón 2003; Leakey and Walker

1985; Ruff 1995). Despite the similarity in size and external gross morphology between KNM-ER 1592 and KNM-ER 736 and 1808, McHenry (1992) suggested that the former should be left unclassified because diagnostic morphological characteristics of *Homo* are not preserved on its external surface. KNM-ER 1592 has since been taxonomically listed as *Homo* sp. (Wood and Leakey 2011).

COMPARATIVE SAMPLES

Fossil Hominins

A list of the comparative fossil hominin femora included in this study is presented in Table 1. The australopith comparative sample includes femora attributed to *Au. afarensis* (A.L. 288-1), *Au. africanus* (StW 99 and 121), and *P. boisei* (OH 80-12). Femora attributed to early *Homo* include *H. habilis* (OH 62), *Homo* sp. (KNM-ER 736, 1472, 1481a, and 1807), East African *H. erectus/ergaster* (KNM-ER 737, 803a, 1808, OH 28), and *H. erectus* from Indonesia (Kresna 11, Trinil II, IV, and V). The East African *H. erectus/ergaster* and Indonesian *H. erectus* samples will be referred to as *H. erectus sensu lato* (Antón 2003). The midshaft femoral morphology in KNM-ER 1472, 1481a, and 1807 has been shown to fit comfortably within the range of variation in early *H. erectus* and early “*erectus*-like” femora, and the proximal femoral morphology in KNM-ER 736 has been shown to align with early *Homo* femora assigned to *H. erectus* or described as “*erectus*-like” (i.e., KNM-ER 737, 803a, 1472,

1481a, 1808, OH 28) (Ruff 1995). As such, the specimens included in the *Homo* sp. group in the current study are considered as likely non-*habilis* *Homo* species. OH 62 was included in this study to provide a non-*erectus* early *Homo* comparison for KNM-ER 1592. However, it was excluded from statistical analyses because all other femora in the early *Homo* comparative sample are considered non-*habilis* or likely non-*habilis* and midshaft femoral diaphyseal morphology is distinct between non-*habilis* early *Homo* and *H. habilis* (Ruff 2009, 1995; Ward et al. 2015). Femora from *H. naledi* (U.W. 101-003, 101-012, 101-268), which have a combination of ancestral traits found in australopithecids (e.g., an anteroposteriorly compressed femoral neck) and shared-derived traits found in early *Homo* (e.g., well-marked linea aspera) (Marchi et al. 2017), are also included because they expand the morphological diversity of the *Homo* lower limb and provide a broader comparative framework for which to compare KNM-ER 1592.

Craniodentally aligned material include the femur from the A.L. 288-1 partial skeleton (Johanson et al. 1982), OH 80-12 (Domínguez-Rodrigo et al. 2013), and three partial skeletons attributed to early *Homo* including OH 62, KNM-ER 803a, and 1808 (Antón 2003; Johanson et al. 1987). All the hominin material from the Dinaledi collection is referred to *H. naledi* and includes cranial and postcranial remains from at least 15 individuals from this newly named species (Berger et al. 2015). The unassociated femora are taxonomically allocated generally following tentative attributions from the published literature (Wood and Leakey 2011) and previous studies based on comparisons with craniodentally associated femora (Ruff 1995). It is important to note that taxonomic attributions for some of the unassociated femora are disputed or problematic. For instance, Wood and Collard (1999) have questioned the inclusion of *habilis* in the *Homo* clade. Although the Trinil femora have historically been classified as *H. erectus*, their attribution to this taxon is uncertain (Antón 2003; Rightmire 1990). Day and Molleson (1973) found the Trinil femora to be strikingly similar to femora from modern humans, and Kennedy (1983b: 613) concluded that while Trinil II and IV shared morphological features with femora assigned to *H. erectus*, their overall morphological pattern aligned them with “the sapients.” Ruff and colleagues (2015) found the morphology of Trinil II, IV, and V to be consistent with early *Homo* (Ruff et al. 2015). Given these disputes and uncertainties, the taxonomic assignments for the craniodentally unassociated femora are best viewed as a means to broadly contextualize the sample for which KNM-ER 1592 is compared against.

Modern Humans

The modern human skeletal series is a convenience sample that consists of the well-preserved remains of females (N= 5) and males (N= 26) from non-archaeological and archaeological contexts across Ontario, Canada. Approximately half of the skeletons (two females and 14 males) are from the Odd Fellows collection and are of unknown provenience (Ginter 2001, 2008). Like other cadaveric skel-

etal collections in North America (e.g., Terry, JCB Grant, and Hamman-Todd), the Odd Fellows collection is male-biased and consists of individuals from the lower echelons of society with generally poor health and a physically demanding lifestyle (Ginter 2008). Other non-archaeological samples included in the modern human series are two male inmates of the Peterborough Jail executed in 1920 (Spence et al. 1999). Individuals from archaeological context include one female and four males from the Stirrup Court cemetery. This cemetery was in use between 1828 to 1890 and consists of residents from a historic peri-urban settlement (Parish 2000). The individuals included in this study likely represent individuals of lower socio-economic status or perhaps farmers (Parish 2000). The remainder of archaeological samples in the modern human series includes two individuals from a 19th century small burial plot near Kitchener, Ontario (Spence 1985), one individual perhaps dating to the 11th century, and another individual dating to the 15th century (Bull and Spence 1988; Molto et al. 1986; Spence 1994). Lastly, four individuals in the modern human series are of unknown provenience. All individuals in this skeletal series were donated to the Department of Anthropology at The University of Western Ontario (now Western University) in London, Ontario, Canada, and are currently housed in that department.

MIDSHAFT CROSS-SECTIONAL RECONSTRUCTION

Beam theory predicts that the most mechanically relevant material is located furthest from the section centroid; therefore, accurate reconstructions of the periosteal contour are paramount for calculating cross-sectional properties (O’Neill and Ruff 2004). Section locations for the modern human femora were taken at 50% of bone length’ measured from the distal end of the bone where length’ refers to bio-mechanical length, which is the bone length used in calculating section locations (Ruff and Hayes 1983). Length’, measured parallel to the longitudinal axis, is defined as the distance between the articulation surface centers of the distal condyles and the superior surface of the femoral neck where the neck meets the greater trochanter just medial to the insertion area for the obturator internus (Ruff and Hayes 1983: 363; Ruff et al. 1999). Cross sections for the modern human femora were reconstructed following the latex cast method (LCM), which uses a combination of silicone molds and bi-planar (i.e., anteroposterior [A-P] and mediolateral [M-L]) radiography to reconstruct subperiosteal and endosteal contours, respectively (Stock 2002). The LCM has been shown to provide a highly accurate estimate of cross-sectional contours and true cross-sectional properties with results accurate to within 5% compared to computed tomography (CT) or direct measurement (O’Neill and Ruff 2004; Ruff 2019: 195; Stock and Shaw 2007). Silicone molds of the subperiosteal surface were made using hydrophilic polysiloxane dental impression material (Exaflex®, GC America Inc.). Endosteal contours were estimated from measurements of cortical wall thicknesses derived from bi-planar radiographs using a Faxitron model 43855A X-ray

machine in the Department of Anthropology at Western University. Section locations were marked with metal wire prior to x-raying, and a scaling device was included in each shot to correct for magnification (Jaundrell-Thompson and Ashworth 1970). Bones were placed in the X-ray machine in standard anatomical position and oriented following methods described by Ruff and Hayes (1983). Diaphyses were leveled by placing pieces of clay under the shaft so that the A-P midpoints of the proximal and distal ends of the bone were equidistant from the image receptor. Kodak T-Mat film was used in Kodak Lanex regular and fast intensifying screens. The source to film distance was 61cm with a focal spot size of 0.5mm. The tube current ranged from 2 to 3mA and the voltage ranged from 60 to 70kVp depending on the sample. Exposure times varied from 3 to 5 seconds. Films were manually processed using Pro Plus® developing and fixing solutions. Digitized radiographic images were enhanced in Adobe Photoshop® and magnified 300–400% to measure anterior, posterior, medial, and lateral cortical wall thicknesses inward from the subperiosteal surface. Cortical wall thicknesses were plotted in correct anatomical position along the A-P and M-L planes on the subperiosteal latex cast tracings without the need for size-adjustment. The anterior, posterior, medial, and lateral points were connected in an ellipse to reconstruct an elliptical medullary cavity (O'Neill and Ruff 2004).

Because the casting putty may leave a residue on bone, subperiosteal casting for KNM-ER 1592 was done on a cast provided by the National Museums of Kenya. External breadths along the transverse and sagittal planes on the cast were cross-checked against external breadth measurements on the original fossil using digital calipers to the nearest 0.01mm. Endosteal contours for KNM-ER 1592 were reconstructed by measuring anterior, posterior, medial, and lateral cortical wall thicknesses using digital calipers to the nearest 0.01mm directly on the fossil. Cortical wall thicknesses were plotted in correct anatomical position on the subperiosteal latex cast tracing without the need for size-adjustment. The endosteal contour was reconstructed by manually connecting the points following the subperiosteal contour. Measurements were taken at the proximal end of the femoral fragment, which is likely to be slightly distal to the midshaft at ~43% given an estimated maximum femur length of 470mm (McHenry 1991). Sládek and colleagues (2010) found that cross-sectional properties (i.e., cortical area and second moments of area) in the midshaft femur of a skeletal sample of modern humans are still accurately estimated (i.e., they have an acceptable mean accuracy range not larger than the accepted error of 5% from the midshaft values) when the exact midshaft location is unknown (sections taken from 40–60% of bone length). They argued that the femoral accuracy range is wide enough for practical application in all biomechanical parameters examined for modern humans, and that individual variation rather than accurate identification of the midshaft was more important when studying fossil hominins with damaged long bones (Sládek et al. 2010: 330). Because the polar section modulus in KNM-ER 1592 is derived from the polar second mo-

ment of area in the current study (see below), presumably the acceptable mean accuracy ranges reported for second moments of area can reasonably be extended to the section modulus. It has also been demonstrated that similar conclusions are attained even when there is variation in the “midshaft” section location at which cross-sectional properties are measured. For instance, Ruff (1995: 569) found that the midshaft femoral morphology in KNM-ER 1807 was closest to femora attributed to early *Homo* (early *H. erectus* and “*H. erectus*-like” specimens). Midshaft properties in KNM-ER 1807 were taken as the averaged properties from the proximal ends of the proximal and distal fragments at ~60–65% and ~40% of length, respectively (Ruff, personal communication). A similar conclusion was reached—that the midshaft femoral morphology in KNM-ER 1807 was most like femora attributed to early *Homo*—when cross-sectional properties were measured on the proximal end of the distal fragment (i.e., at ~40% of length) (Bleuze 2010). It is widely recognized and accepted that section locations are often approximations when studying fossil long bones, especially when they are fragmented (Ruff 1995). Thus, while it is acknowledged that the cross-sectional properties in KNM-ER 1592 are not taken exactly at the midshaft, it is unlikely that minimal section location error (i.e., measurements taken at ~43% rather than at 50%) will have a significant impact on the overall patterns and general conclusions attained. A possible exception may be with M-L bending rigidity and strength relative to A-P bending rigidity and strength or diaphyseal shape. Proportions of bending rigidity and strength in the anatomical planes are known to change along the femoral diaphysis with M-L bending rigidity and strength relative to A-P bending rigidity and strength increasing in sections distal to the midshaft in later *Homo* (e.g., Middle Paleolithic and Early and Mid-Upper Paleolithic modern humans) and decreasing in sections distal to the midshaft in earlier *Homo* (e.g., Early and Middle Pleistocene) (Trinkaus and Ruff 2012: 25, Figure 8).

Reconstructed cross-sectional tracings for the modern human series and KNM-ER 1592 were digitized using a Lexmark X 6170 flatbed scanner. A scaling device was included to ensure that the size of the images was not compromised during digitization. The images were imported into NIH ImageJ (<https://imagej.nih.gov/ij/>) and cross-sectional properties were calculated using a Macintosh version of MomentMacro written for ImageJ (<http://www.hopkinsmedicine.org/fae/mmacro.html>). All digital and osteometric measurements and cross-sectional properties were calculated three times and the average was recorded. The digitized cross-sectional outline for the mid-diaphyseal section in KNM-ER 1592 is shown in Figure 1.

CROSS-SECTIONAL PROPERTIES

Data for the comparative fossil hominin samples were derived from previous studies (Domínguez-Rodrigo et al. 2013; Friedl et al. 2019; Puymerail et al. 2012; Ruff 2009; Ruff et al. 2015; Ruff et al. 2016; Ruff et al. 2020; Trinkaus and Ruff 2012). Total area (*TA* mm²) refers to the total subperiosteal area of the cross section, and cortical area (*CA*

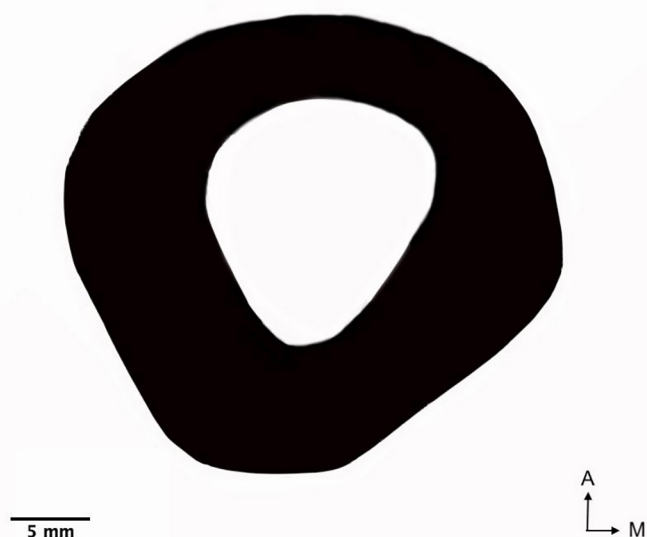


Figure 1. Cross-sectional outline for the femoral mid-diaphysis in KNM-ER 1592.

mm²) is the amount of cortical bone within the cross section. Second moments of area (SMAs mm⁴) quantify the distribution of material along a specific plane about a defined axis and are proportional to the bending rigidity of the section about that axis (Ruff 2019). Rigidity is the internal resistance of a structure to an externally applied force or mechanical load (Reilly and Burstein 1974). The SMA about the M-L plane, I_x , provides a measure of bending rigidity in the A-P plane and the SMA about the A-P plane, I_y , provides a measure of bending rigidity in the M-L plane (Ruff 2019). The sum of any two perpendicular SMAs (e.g., $I_x + I_y$) is equal to the polar second moment of area, J , which is proportional to torsional and average bending rigidity in cross sections that do not radically depart from circularity (Ruff 2019).

Section moduli (mm³) are considered the best estimates of average bending and torsional strength when mechanical loading conditions are unknown (Ruff 2008). Strength is the maximum stress sustained by a structure before failure (Reilly and Burstein 1974). The polar section modulus, Z_p , is a measure of torsional and average bending strength (Ruff 2019). It is less dependent on the precise orientation of the section location along the anatomical axes and is therefore preferred for use with fragmentary fossil remains, which are often difficult to orient in correct anatomical position (Ruff 2009). When comparing or combining datasets, it is important to consider the method by which section moduli were derived because various methods give slightly, albeit significantly, different results (e.g., true section moduli calculated from various software programs are always less than or equal to section moduli derived from a radius) (Ruff 2008, 2019). Polar section moduli for the modern human series and KNM-ER 1592 were calculated from SMAs based on the formula provided in Trinkaus and Ruff (2012: 55) because most of the comparative fossil hominin data were derived from that study. For the remaining compar-

ative fossil hominin femora, Z_p was approximated either by taking J to the power of 0.73 ($J^{0.73}=Z_p$) or by dividing J by half the external breadth (radius) following Ruff (1995, 2008), or true Z_p was calculated from various software programs (see references in Table 2 for more details). Midshaft femoral cross-sectional properties for the fossil samples are presented in Table 2.

DATA ANALYSES

Because body size constitutes a mechanical load and is related to other factors that influence mechanical loading (e.g., muscle size), it is necessary to account for differences in body size when comparing cross-sectional geometric properties among individuals and populations (Ruff 2019). In biomechanical studies, CA is best standardized by body mass because it is related to pure axial loadings, while properties that measure bending and torsion (e.g., SMAs and section moduli) are best standardized to the product of body mass and beam length (approximated by bone length) because they involve a force (body mass) and a moment arm or distance (bone length) (Ruff 2000, 2019). Body mass estimates appropriate for the present study, however, are unavailable for many of the specimens, including KNM-ER 1592. This is because published body mass estimates for fossil hominin femora lacking their proximal and distal articular ends were based on diaphyseal breadths or circumference (e.g., McHenry 1992 for KNM-ER 1592 and 1807) making them unsuitable under the current context given that the use of the same or related skeletal parameters under study to estimate body mass is circular reasoning (Ruff et al. 1993, 2018). Powers of bone length can also be used to standardize cross-sectional properties to body “size” (Ruff 2019). Such procedures, however, can provide spurious results that reflect differences in limb length between groups rather than differences in “standardized” diaphyseal properties (Holliday 2002). In addition, standardizing cross-sectional properties by powers of bone length assumes similar body shape among the individuals under study (Ruff et al. 1993; Ruff 2019), which is likely not the case in the present study given the geographical and temporal diversity of the comparative fossil sample and modern human series. Given these limitations, data were analyzed in a way that did not require size standardization of cross-sectional properties.

The relationships between CA and TA and I_y and I_x were examined in Ln-Ln scatter plots. Natural log transformation of cross-sectional properties is commonly done to maintain proportionality across variation in size. The distribution of CA for a given TA provides an indication of differential development because this relationship reflects the differential patterns of independent bone deposition and resorption that typically occur on opposite bone envelopes or surfaces (e.g., endosteal resorption and subperiosteal deposition), and is also informative from a structural perspective because CA provides a measure of resistance to axial loads (Ruff et al. 1993; Ruff 2019). The relationship between I_y and I_x provides an indication of differential bending rigidity along the anatomical planes of the femur. This lends

TABLE 2. MIDSHAFT FEMORAL CROSS-SECTIONAL PROPERTIES IN FOSSIL SAMPLES.

Sample	Cross-sectional properties ^a						Source ^b
	TA	CA	I_x	I_y	J	Z_p	
KNM-ER 736	871	659	56553	60075	116628	5496	1
KNM-ER 737	586	441	21538	32802	54340	3165	1
KNM-ER 803a	626	504	27573	34793	62366	3598	1
KNM-ER 1472	464	400	16191	17987	34178	2303	1
KNM-ER 1481a	391	332	10167	14416	24583	1847	1
KNM-ER 1807	636	512	29884	32514	62397	3701	2
KNM-ER 1808m, n	551	478	20813	27251	48064	3006	1
KNM-ER 1592	715	519	31727	37922	69649	4117	this study
OH 28	576	410	18731	31758	50489	3077	1
OH 62	265	220	5294	5700	10995	1154	3
OH 80-12	526	492	21763	22161	43924	2450	4
AL 288-1	330.1	197.6	7221	7327	14548	13050	5
StW 99	484	356	35460	15121	20339	2518	6
StW 121	363	292	20328	10982	9346	1653	6
U.W. 101-003	351	265.1	9181	9401	18582	1571	7
U.W. 101-012	289	249.9	7887	5624	13510	1237	7
U.W. 101-268	361.4	296.6	11538	8850	20388	1696	7
Trinil II	559	406	23622	22891	46513	3423	8
Trinil IV	521	393	18916	26237	44153	3327	8
Trinil V	491	349	15008	22289	37297	2858	8
Kresna 11	590	454	23587	30201	53789	3748	9

^aTA=total subperiosteal area (mm²), CA=cortical area (mm²), I_x =second moment of area about the mediolateral (M-L) plane (mm⁴), I_y =second moment of area about the anteroposterior (A-P) plane (mm⁴), J=polar second moment of area (mm⁴), and Z_p =polar section modulus (mm³). Trinkaus and Ruff (2012) estimated Z_p from the formula $Z_p = ((J/((A-P + M-L)/4)) \times 0.842) + 115$. The same formula was used to estimate Z_p in KNM-ER 1592. The polar section modulus was not reported for OH 80-12 but J was reported, so the former was estimated as $J^{0.73}$. For OH 62, Z_p was estimated as J divided by the average radius of the section (Ruff 2009). For the remaining samples, true Z_p was calculated using various software.

^bSources where the comparative data were derived: 1. Trinkaus and Ruff (2012); 2. Ruff (personal communication); 3. Ruff (2009); 4. Domínguez-Rodrigo et al. (2013); 5. Ruff et al. (2016); 6. Ruff et al. (2020); 7. Friedl et al. (2019); 8. Ruff et al. (2015); 9. Puymerail et al. (2012).

insight into diaphyseal shape, which is influenced by morphological contours on the subperiosteal surface and functional adaptations of the lower limbs due to biomechanical effects (Ruff 2019). Second moments of area about the anatomical planes were examined rather than section moduli along the anatomical planes (i.e., Z_x and Z_y) because true I_x and I_y were available in all the comparative samples.

Reduced major axis (RMA) regression lines were plotted for each group, but lines were compared only between the modern human and early *Homo* groups because each has a sample size large enough for meaningful interpretation. This was done to visualize and interpret patterns in KNM-ER 1592 more easily. R was used to conduct statistical analyses (v4.1.2; R Core Team 2021). The *lmodel2* function in the *lmodel2* package was used to compute RMA regression lines (standard major axis [SMA] in R) (Legen-

dre 2018), and the *slope.com* and *elev.com* functions in the Standardised Major Axis Tests and Routines (*smatr*) package were used to test for common slopes and elevations between the regression lines (Warton et al. 2012). If lines are not parallel (i.e., slopes are significantly different), then the relationship between the two variables under consideration is different between the two groups. The elevations of the lines were not tested if slopes were significantly different. If lines were parallel, then elevations were tested to assess how the regression lines were shifted up or down on the *y*-axis. The significance level was set to 0.05. The *plot* and *abline* functions in the *graphics* package were used to create scatter plots and plot RMA lines, respectively. RMA lines were plotted using the *sma* function from the *smatr* package with the *abline* function.

The *boxplot* function in the *graphics* package was used to

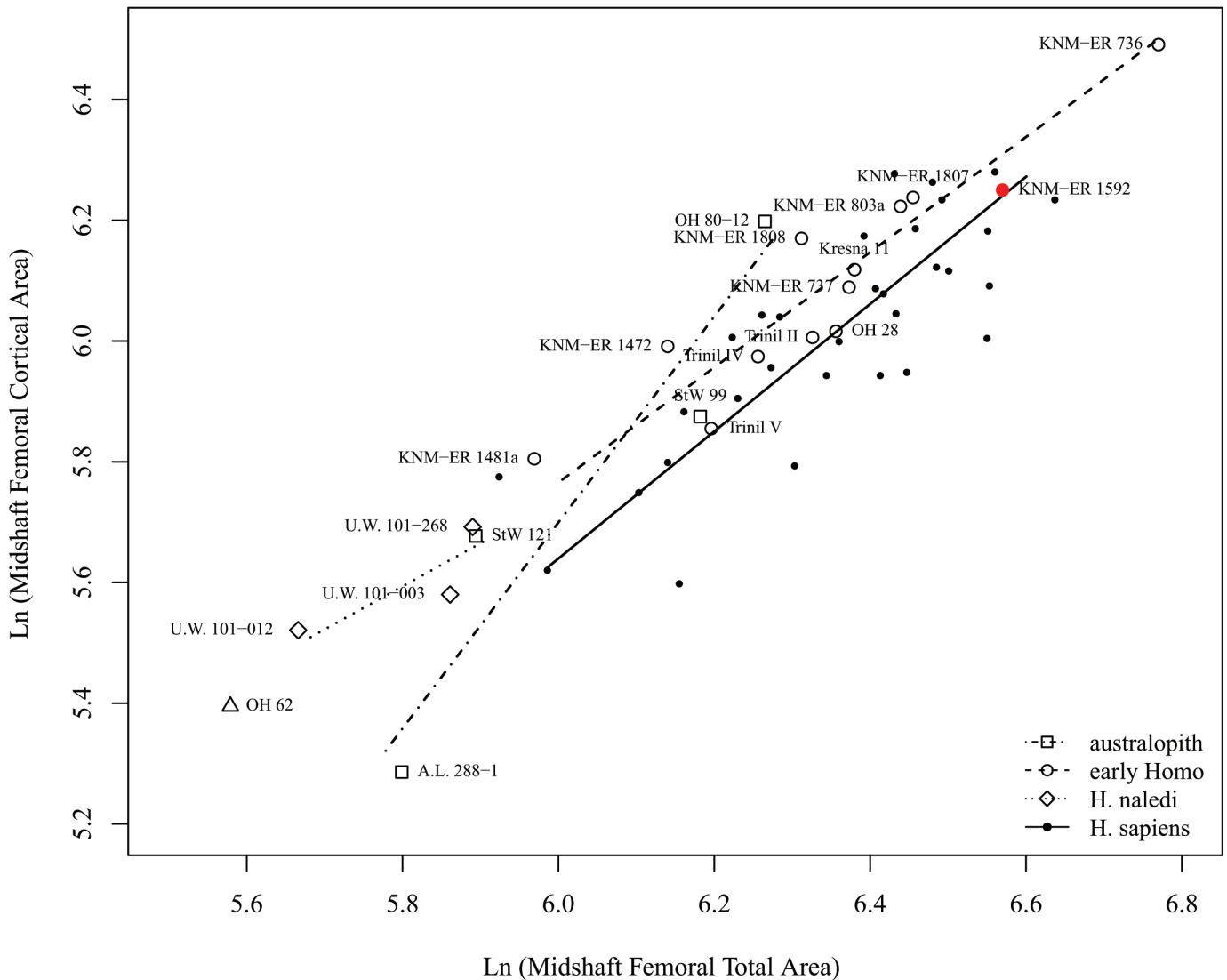


Figure 2. Bivariate scatter plot of natural log-transformed cortical area on natural log-transformed total area in the midshaft femur. Reduced major axis (RMA) lines are plotted for each group. The early *Homo* regression line was constructed without OH 62 (see text for explanation). OH 62 was plotted to provide a non-erectus early *Homo* comparison for KNM-ER 1592.

construct a box plot of Z_p for the australopith, early *Homo*, and *H. naledi* groups. Z_p in KNM-ER 1592 was visually compared to the distributions in the fossil hominin groups to further examine it in comparative context.

RESULTS

Slopes are not statistically significantly different between the modern human and early *Homo* groups for CA regressed on TA ($p=0.40$) and for I_y regressed on I_x ($p=0.19$). There is significantly greater CA for a given TA in the midshaft femur of early *Homo* compared to modern humans ($p=0.01$) (Figure 2). Cortical area for a given TA is also elevated in KNM-ER 1592 compared to the modern human series, but it falls comfortably within the spread of non-*habilis* early *Homo* and modern human data points. While not as large as KNM-ER 736, KNM-ER 1592 is of considerable size compared to other specimens and is most similar to KNM-ER

803a and 1807 in this regard. The relationship between CA and TA at the midshaft femur alone may not be a strong diagnostic trait to infer the taxonomic identity of KNM-ER 1592 given the overlap of some australopiths, particularly StW 99 and to some extent OH 80-12, with early and modern *Homo*. However, when size is also considered KNM-ER 1592 is more consistent with non-*habilis* early *Homo* than with the australopiths.

Early *Homo* femora show significantly greater M-L bending rigidity for a given A-P bending rigidity in the midshaft section compared to modern human femora ($p<0.01$), although there is a lot of overlap between the early *Homo* and modern human data points (Figure 3). This is mainly due to the considerable variation in the modern human series. There is a lot of variation among the australopiths as well with OH 80-12 falling with modern humans, StW 121 falling with *H. naledi*, and StW 99 falling with early

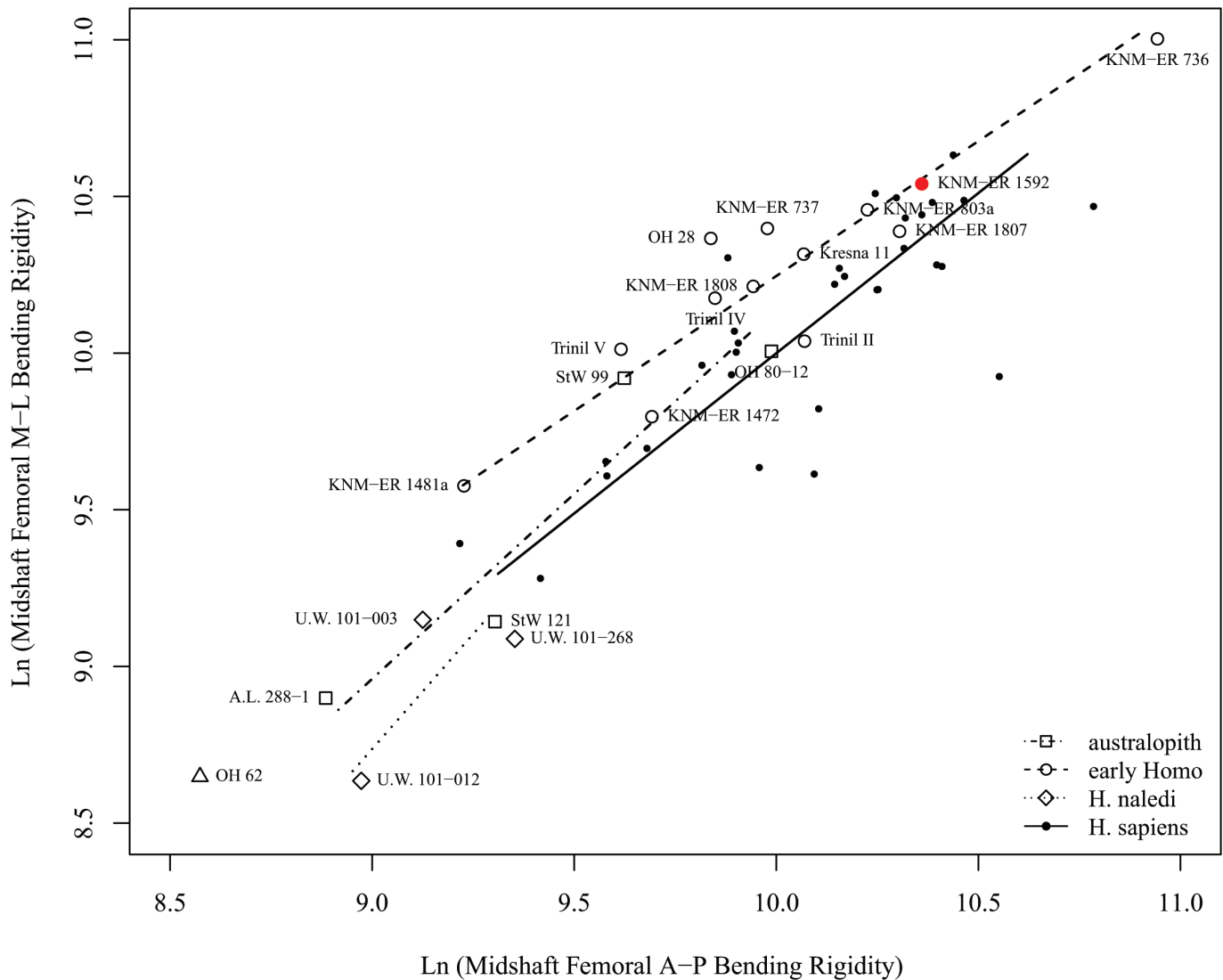


Figure 3. Bivariate scatter plot of natural log-transformed mediolateral (M-L) bending rigidity on natural log-transformed antero-posterior (A-P) bending rigidity in the midshaft femur. Reduced major axis (RMA) lines are plotted for each group. See Figure 2 regarding OH 62.

Homo. KNM-ER 1592 falls on the early *Homo* regression line and displays the greater M-L relative to A-P expanded mid-diaphyseal morphology characteristic of *H. erectus* and “*erectus*-like” femora.

Visual summaries of the distribution of Z_p in australopiths, early *Homo*, and *H. naledi* with the value in KNM-ER 1592 plotted further demonstrate its affinity with non-*habilis* early *Homo* (Figure 4). Some early *Homo* femora have Z_p values that overlap with the australopith distribution, but most, including KNM-ER 1592, have Z_p values that are well above those observed in the australopiths.

DISCUSSION

The overall morphology of the mid-diaphyseal femur in KNM-ER 1592 allies it with Pleistocene femora attributed to *Homo*, specifically non-*habilis* early *Homo*. This includes KNM-ER 803a and 1808 which have been craniodentally

aligned with *H. erectus sensu lato* (Antón 2003), and femora that have been assigned to *H. erectus* or described as “*erectus*-like” based on morphometric comparisons with femora associated with diagnostic craniodental material (Ruff 1995). An expanded M-L diameter relative to A-P diameter in the midshaft femoral diaphysis is a key feature of *H. erectus* from East Africa and Java that is not observed in femora attributed to *H. habilis* (Ruff 1995, 2009; Ruff et al. 2015; Ward et al. 2019). KNM-ER 1592 displays a greater M-L diameter relative to A-P diameter consistent with non-*habilis* early *Homo* and is clearly distinct from OH 62 in this regard. Torsional and average bending strength in KNM-ER 1592 is more compatible with observations in *H. erectus* and “*erectus*-like” femora than with observations in the australopiths and OH 62. The alignment of KNM-ER 1592 with non-*habilis* early *Homo* is further supported when size, both overall cross-sectional size and estimated femur

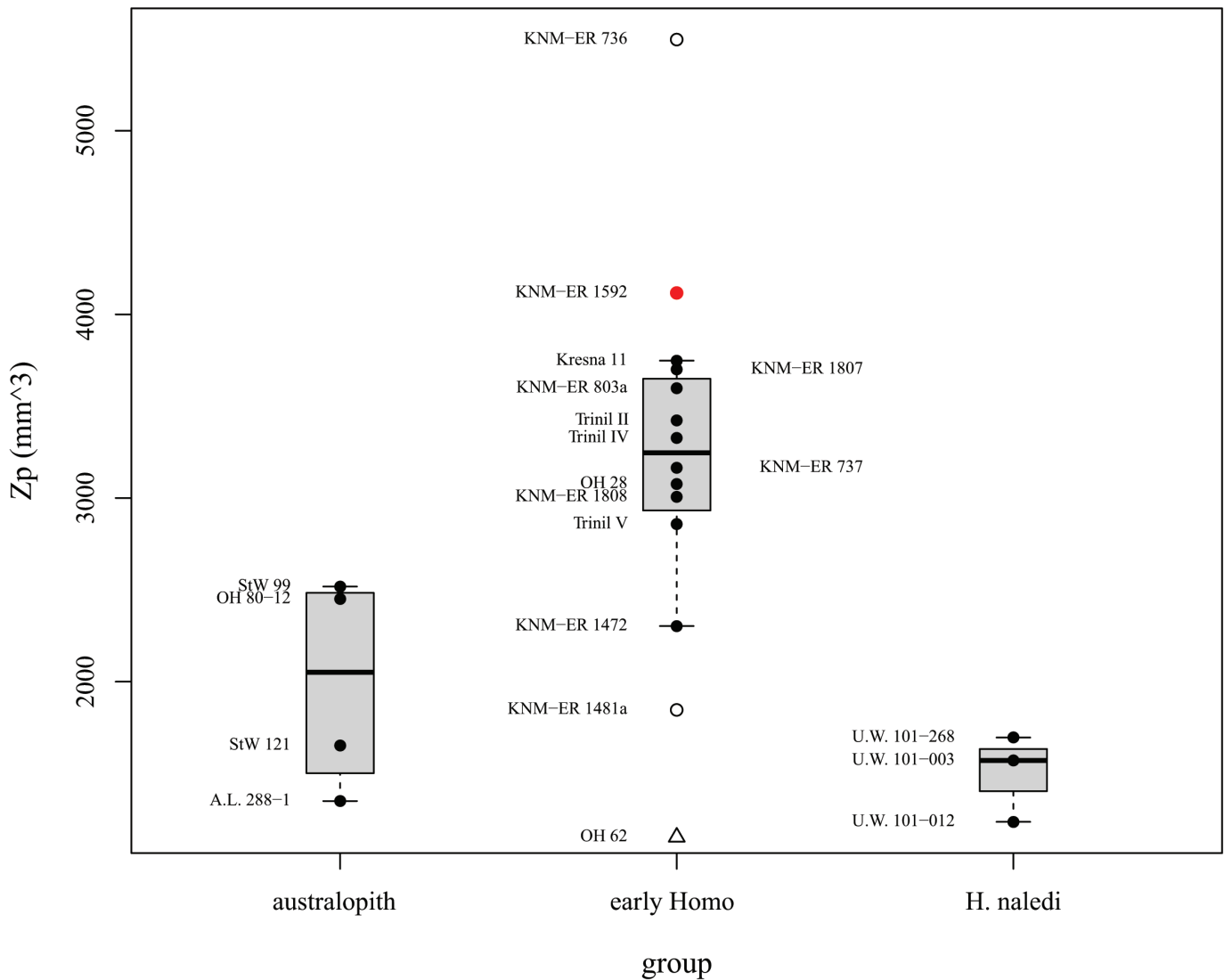


Figure 4. Box plot of Z_p in australopiths, early Homo, and *H. naledi*. The bottom and top of the box represent the 25th and 75th percentiles (or first [Q1] and third [Q3] quartiles), respectively, and the box represents the interquartile range (IQR= Q3 – Q1). The horizontal bar inside the box represents the median (50th percentile). The upper and lower whiskers extend to the maximum and minimum values, respectively, that are not outliers. Outliers are data points that fall more than 1.5 times the IQR and are marked as open circles. The box plot for the early Homo sample was constructed without OH 62 (see text for explanation). The Z_p value in OH 62 was plotted to provide a non-erectus early Homo comparison for KNM-ER 1592.

length (McHenry 1991), is also considered. Although there is overlap in cross-sectional size among some australopith and fossil *Homo* samples at the smaller (e.g., OH 62, the *H. naledi* femora, StW 121, and A.L. 288-1) and intermediate (e.g., KNM-ER 1472, Trinil V, and StW 99) size ranges, australopith and fossil *Homo* samples do not overlap at the larger end of the size range where KNM-ER 1592 consistently falls with KNM-ER 803a, 1807 and, to a lesser extent, KNM-ER 736, which is easily the largest specimen included in this study. To summarize, KNM-ER 1592: 1) has a mid-diaphyseal femur reinforced in terms of relative cortical thickness placing it within the range of variation observed in modern humans and Pleistocene non-*habilis* early *Homo*; 2) displays greater bending rigidity in the M-L plane for

a given bending rigidity in the A-P plane more consistent with patterns observed in non-*habilis* early *Homo*; 3) has a Z_p value more consistent with *H. erectus* and “erectus-like” specimens than with australopiths and OH 62; and, 4) has an overall cross-sectional size and estimated femur length that are more *Homo*-like than australopith-like. Together, mid-diaphyseal femoral morphology and overall size in KNM-ER 1592 suggest a closer alignment with *Homo*, specifically non-*habilis* early *Homo*, than with *Australopithecus* or *Paranthropus* based on the comparative data set in this study.

The midshaft femur in Pleistocene *Homo* is characterized by a significant increase in relative cortical area when compared to the same section in modern humans (i.e., fos-

sil *Homo* midshaft femora have relatively thicker cortices than those of modern humans) (Ruff 1995; Ruff et al. 1993; Trinkaus and Ruff 1999). This cross-sectional geometric morphology has been suggested to possibly reflect an increase in overall mechanical loading in the postcranial skeleton in pre-modern *Homo* compared to modern humans, albeit the direct mechanical significance of increased relative CA is not well understood (Ruff 1992; Ruff et al. 1993). Since the relationship between CA and TA reflects the differential endosteal resorption and subperiosteal deposition that occurs primarily during ontogeny and, to a lesser extent, throughout adulthood, and since the subperiosteal and endosteal surfaces respond to increased mechanical loading differently during development, it is necessary to consider the potential impact of different ontogenetic trajectories in modern humans and fossil hominins when interpreting cross-sectional diaphyseal morphology (Bertram and Swartz 1991; Feik et al. 2000; Pearson and Lieberman 2004; Ruff et al. 1994; Trinkaus and Ruff 2012). Indeed, the relatively thicker cortices in the femur of juvenile pre-modern humans (*H. erectus sensu lato* and Neandertals) compared to their modern age-matched counterparts (Ruff et al. 1994) and the excessive relative cortical bone reinforcement in the femur of adult pre-modern humans (*Homo* sp., *H. erectus sensu lato*, Neandertals, and early modern *H. sapiens*) beyond what would be structurally necessary for a given body mass (Ruff et al. 1993) allude to some genetic (developmental) influence on relative cortical thickening in the femur. The relationship between CA and TA in the midshaft femur of KNM-ER 1592 is consistent with patterns observed in Pleistocene femora attributed to genus *Homo*, which may indicate a similar pattern in axial loading in the postcranial skeleton and/or comparable ontogenetic trajectories which affect when and how rapidly cortical bone is deposited and resorbed in the subperiosteal and endosteal surfaces (Feik et al. 2000).

Diaphyseal cortical thickness in australopith femora can match or exceed values in early *Homo* femora thereby minimizing the usefulness of this trait for distinguishing between early *Homo* and some non-*Homo* femora (Domínguez-Rodrigo et al. 2013). Indeed, CA to TA in OH 80-12 and StW 99 fall within the variation observed in the non-*habilis* early *Homo* and modern human groups. The limited value of CA to TA for helping to differentiate early *Homo* from non-*Homo* femora is further demonstrated when percent CA is explored. Percent CA ($\%CA = (CA/TA) \times 100$) can be used to describe the relative cortical thickness from a strictly morphological rather than biomechanical perspective because it does not have a direct mechanical significance (Ruff 2019). The %CA in the midshaft femur of KNM-ER 1592 is 72.59%, which falls within the ranges for the australopith (59.86%–93.54%) and non-*habilis* early *Homo* (71.08–86.75%) groups whose ranges also overlap. Midshaft %CA in KNM-ER 1592 is not exactly comparable with values taken at the actual midshaft (50%) because the mid-diaphyseal section in KNM-ER 1592 is at ~43%. Relative CA in the femur tends to decrease distal to the midshaft (Trinkaus and Ruff 2012), so if anything, the %CA in KNM-

ER 1592 at ~43% is probably slightly lower than its %CA at its true midshaft. Thus, while the relationship between CA and TA in KNM-ER 1592 is comparable to patterns in non-*habilis* early *Homo* and modern humans, this trait alone is not strong enough evidence to argue for an alignment with genus *Homo* because some australopiths (e.g., OH 80-12 and StW 99) also overlap with the variation in these *Homo* groups.

Diaphyseal cross-sectional shape reflects subperiosteal contours, which are influenced by morphology (e.g., the presence of a midshaft pilaster, development of a medial buttress), and habitual biomechanical loading, which alters the distribution of bone tissue along the anatomical planes of the diaphysis (Ruff 2019). Compared to modern humans, the proximal to midshaft femur in *H. erectus sensu lato* is known to show an increase in M-L bending rigidity and strength for a given A-P bending rigidity and strength (Ruff 1995; Ward et al. 2015). The finding of early *Homo* midshaft femora showing significantly greater M-L bending rigidity for a given A-P bending rigidity compared to modern humans presented here was, therefore, not unexpected. Anatomical traits in the proximal femur and pelvis, especially a relatively long femoral neck, more laterally flared ilia, and an increase in bi-iliac and bi-acetabular breadths, contribute to increased M-L bending rigidity and strength to A-P bending rigidity and strength in the midshaft femur (Lovejoy et al. 2002; Ruff 1995; Shaw and Stock 2011). However, while many australopiths also have a relatively long femoral neck (Lovejoy and Heiple 1972) and a platypelloid pelvis (Rosenberg and Trevathan 1995) they tend to show only a moderate increase in M-L bending rigidity and strength to A-P bending rigidity and strength in the midshaft femur when compared to *H. erectus sensu lato* and fall well within the range of variation in modern humans (Ruff et al. 1999, 2020). Thus, the distinct increase in M-L bending rigidity and strength to A-P bending rigidity and strength in the midshaft femur of *H. erectus sensu lato* is likely explained by the suite of morphological features in the proximal femur and pelvis and biomechanical effects (e.g., gait) (Ruff et al. 2020). Without the proximal femur and pelvis, it is not possible to assess the influence of proximal femoral and pelvic morphology on midshaft femoral diaphyseal shape in KNM-ER 1592. However, if KNM-ER 1592 had a similar proximal femoral and pelvic morphology as early *Homo* and the australopiths but had a more australopith-like gait, then it would be expected to display a moderate increase in M-L bending rigidity to A-P bending rigidity overlapping with the variation in modern humans as has generally been observed in the midshaft femur of australopiths (Ruff et al. 2020). Instead, the differential bending rigidity in the anatomical planes of the midshaft femur in KNM-ER 1592 is consistent with patterns in non-*habilis* early *Homo*, which possibly indicates comparable gait mechanics (assuming a similar proximal femoral and pelvic morphology as non-*habilis* early *Homo*) lending support to its taxonomic alignment more with genus *Homo* than with an australopith genus.

Diaphyseal shape is known to change along the fem-

oral diaphysis in fossil and modern hominins (Ruff 1987; Ruff et al. 2020; Trinkaus and Ruff 2012). Trinkaus and Ruff (2012) found that diaphyseal shape became less expanded in the M-L diameter relative to the A-P diameter from the midshaft (50%) to the mid-distal (35%) section in six early Pleistocene *Homo* femora from East Africa (KNM-ER 736, 737, 803a, 1472, 1481a, and 1808). Given that measurements in KNM-ER 1592 were taken slightly distal to its midshaft, it is probable that diaphyseal shape in this specimen might be different than at its actual midshaft. Trinkaus and Ruff (2012) used diaphyseal landmarks to approximate section locations in the majority of the early Pleistocene femora from Koobi Fora in their study given the fragmentary nature of the specimens. The maximum extent of the pilaster and the narrowest shaft breadth were used to approximate the midshaft (Trinkaus and Ruff 2012). They acknowledged that the midshaft section was less clearly indicated morphologically in pre-modern humans compared to modern humans because the former lack a pilaster and frequently show prominent medial buttressing, and suggested that diaphyseal shape changes little along several centimeters of the midshaft such that “modest errors in the location of the 50% section should introduce little error into the values,” (Trinkaus and Ruff 2012: 16). Thus, while it is recognized that the “midshaft” diaphyseal shape in KNM-ER 1592 reported here is probably somewhat different than at its true midshaft it is unlikely to significantly alter interpretations of its place in comparative context with other hominin femora.

The development of a well-defined pilaster is a distinguishing feature in the modern human femur, and it is usually absent or poorly developed in pre-modern *Homo* (Ruff 1995; Trinkaus 1997; but see Haeusler and McHenry 2004 and Ward et al. 2015 for *H. habilis*, and Marchi et al. 2017 for *H. naledi*). The decreased M-L to A-P cross-sectional diaphyseal shape in the midshaft femur of modern humans compared to fossil *Homo* has been attributed, in part, to the presence of a true, well-developed pilaster in early and recent *H. sapiens* and perhaps to the increased M-L oriented bending loads in the proximal to midshaft femur in fossil *Homo* compared to modern humans (Rodríguez et al. 2018). Interestingly, KNM-ER 1592 exhibits a “strong pilaster that swings towards the lateral condyle distally” (Leakey and Walker 1985: 137–138), yet it still maintains the midshaft cross-sectional diaphyseal shape characteristic of fossil *Homo*—an elongated M-L to A-P section. This may further support the conjecture that KNM-ER 1592 potentially had comparable gait mechanics and proximal femoral and pelvic morphology to non-*habilis* early *Homo*. Although a strong pilaster is not a defining feature of the femur in early *Homo*, it has been observed in some femora attributed to *H. habilis* or non-*erectus* early *Homo* including OH 62 and KNM-ER 3735 and 5881a but its development may be related to the reduced M-L diameter relative to A-P diameter near the midshaft in these specimens (Ruff 1995; Ward et al. 2015). While KNM-ER 1592 has a pilaster, whether strongly developed as described by Leakey and Walker (1985) or weakly developed as shown in Figure 1 in this study, this

by itself does not support an affiliation with *H. habilis* or non-*erectus* early *Homo* given its relatively expanded M-L diameter near the midshaft and overall size. In addition, the Z_p value in KNM-ER 1592 further demonstrates its affinity with non-*habilis* early *Homo*.

The overlap of the Sterkfontein femora with *Homo* complicates attempts to taxonomically identify KNM-ER 1592 based on structural analyses because these femora make inter-taxonomic differences less decidedly distinct between *Homo* and *Australopithecus*. StW 99 and 121 have a proximal femoral morphology consistent with other australopiths, but the early “*erectus*-like” morphology at the midshaft in StW 99 is unusual (Ruff et al. 2020). Ruff and colleagues (2020) suggested that the “*erectus*-like” morphology at the midshaft may have functional implications related to bio-mechanical loading around the hip. They noted, however, that the “midshaft is less informative regarding load transfer around the hip, and by extension, pelvic shape, and bipedal locomotion,” so the “*erectus*-like” morphology at the midshaft “carries less weight in terms of biomechanical inferences,” than does the morphology in the proximal femur (Ruff et al. 2020: 316). Perhaps, then, it is possible that the “*erectus*-like” morphology at the femoral midshaft in StW 99 indicates that this femur is a representative of genus *Homo* rather than an australopith. Grabowski and colleagues (2015: 90) noted that the original catalog states that StW 99 comes from Sterkfontein Member 5 (1.6–1.1 Ma), which has yielded *P. robustus* and early *Homo* specimens (Partridge et al. 2003). Based on the age of this member and their visual inspection of the morphology of StW 99, they suggested that StW 99 is more likely to be early *Homo* than *Au. africanus* (Grabowski et al. 2015: 90). Pickering and colleagues (2021: 7) suggested that StW 99 may likely be a *Paranthropus* specimen “given its morphological continuity with the Swartkrans *Paranthropus* femur fossils and its possible origin from the *Paranthropus*-bearing Member 5 unit of the Sterkfontein Formation.” Alternatively, it is possible that StW 99 is in fact an australopith but variation in australopith midshaft femoral morphology may be so broad that it precludes attempts to identify a uniquely australopith pattern. Although the catalog where StW 99 is housed lists the fossil as deriving from Member 5, the grid location where it was recovered is clearly within the boundary of Member 4 (DeSilva and Grabowski 2020) and Member 4 hominin material is usually assigned to *Au. africanus* because this is the primary species in this unit (Partridge et al. 2003). High morphological variation within the Member 4 assemblage may indicate taxonomic heterogeneity with possibly more than one species of australopith represented (Clarke 1985; Fornai et al. 2021) or high intraspecific variation in *Au. africanus* perhaps in relation to temporal heterogeneity (Grine et al. 2013). Harmon (2009: 558) suggested that size variation in the proximal femur of 11 adult *Au. africanus* samples, including StW 99, was consistent with a single species, but the possibility exists that multiple species are present in the sample based on the degree of variation in some shape variables (e.g., femoral head diameter, neck height, neck breadth). She found that StW 99 had a

longer femoral neck and a smaller femoral head than the other *Au. africanus* femora, and that the shape variation in the proximal femoral morphology among *Au. africanus* samples was moderate to high and increased when specific *Au. africanus* femora, including StW 99, were included in the analyses (Harmon 2009). While the taxonomic status of StW 99 is not the focus of the current study, it is relevant to note that some aspects of its morphology, both proximally (Harmon 2009) and at the midshaft (Ruff et al. 2020), are distinct from other australopiths and, more specifically, other *Au. africanus* samples. If StW 99 is indeed a representative of *Au. africanus*, observations of it falling within the spread of *Homo* data points for CA to TA and I_y to I_x may not necessarily mean that *Au. africanus* and *Homo* cannot be distinguished based on these bivariate relationships given that StW 99 appears to be unusual in both cross-sectional morphology and overall size for an australopith (Ruff et al. 2020). The inclusion of additional femora attributed to *Au. africanus* may help clarify similarities and differences in midshaft cross-sectional geometry between *Au. africanus* and *Homo*.

The femur serves as a weight-bearing structure during stance and locomotion, and because bone responds to habitual, mechanical loading throughout life, femoral diaphyseal shape and structure can give some indication of function during life (Martin and Burr 1989). While this is precisely the reason limb bone cross-sectional properties can be used to reconstruct habitual behaviors in individuals and past populations (Ruff 2019), their plastic nature may limit their use in taxonomic identification. However, given the assertion that a genus should include species that occupy a single consistent and coherent adaptive zone (Wood and Collard 2001: 67), plasticity in midshaft femoral structure in response to mechanical loading is not necessarily a hindrance to taxonomic identification, specifically to the genus level. Midshaft femoral diaphyseal structure can provide insight into locomotor behavior in fossil hominins (e.g., Ruff 2009; Ruff et al. 2016, 2020) and locomotor behavior constitutes an important part of a species' adaptive strategy (Wood and Collard 2001). Because genetic and mechanical (environmental) influences are inseparable and equally important for understanding diaphyseal morphological variation (Ruff et al. 2006) and because locomotor behavior can be considered a critical aspect for inclusion in a genus (Wood and Collard 2001), plasticity in midshaft femoral diaphyseal shape resulting from mechanical loading does not diminish its use for testing hypotheses about the generic identity of isolated femora.

Evolutionary adaptations in response to selective pressures and the impact of genetic background on bone structure independent of functional loading histories are also important factors to consider when interpreting diaphyseal structure (Bertram and Swartz 1991; Wallace et al. 2010, 2017). For instance, similar selective pressures on pelvic morphology in different taxa may make it difficult to taxonomically identify different groups based on femoral diaphyseal morphology. It has been suggested that the M-L pelvic breadth in *H. habilis* may have been more like

that observed in the australopiths than in *H. erectus* and "erectus-like" specimens given the nearly circular proximal diaphyseal shape in *H. habilis* (OH 62) which is more akin to patterns in *Australopithecus* than to patterns in other *Homo* specimens (Ruff 1995). Evolutionary adaptations in pelvic morphology, however, are less influential on the midshaft region than on the proximal region of the femoral diaphysis (Ruff 1995). Given the midshaft femoral diaphyseal morphology in KNM-ER 1592 is similar to *H. erectus* and "erectus-like" specimens and the clear distinctions in mid-diaphyseal morphology between australopith and *H. habilis* versus *H. erectus*/"erectus-like" femora, the use of midshaft femoral diaphyseal morphology remains valuable for distinguishing among an australopith, *H. habilis*, and non-*habilis* early *Homo*. Ontogenetic influences may also present another challenge when interpreting femoral diaphyseal structure (Pearson and Lieberman 2004). While ontogenetic influences on diaphyseal structure are well recognized (Ruff 2019; Ruff et al. 1994), such influences may be irrelevant here because known juvenile specimens were excluded from the study. Although the absence of articular ends in many of the fossil hominin femora in this study, including KNM-ER 1592, makes it difficult to definitively rule out the presence of juveniles, the overall size of these femora suggests adult status. Biomechanical analyses must be applied with appropriate caution when attempting to assign isolated femora to a taxon particularly in the absence of the proximal and distal portions of the bone, which contain additional diagnostic characteristics of value for helping to ascertain taxonomic identity. Thus, while the structural analyses of the mid-diaphysis in KNM-ER 1592 suggest an assignment to genus *Homo* is reasonable, this recommendation must be considered tentative.

CONCLUSIONS

Reconstructing hominin evolution requires accurate taxonomic placement of fossil material, which can be a challenge for isolated postcranial remains because taxonomic identity is traditionally based on craniodental morphology. Biomechanical analyses have been instrumental in providing an avenue for which to test hypotheses about the taxonomic identity of isolated postcranial material. Cross-sectional geometric properties in the mid-diaphysis in KNM-ER 1592 indicate morphometric, and by implication biomechanical, similarities with Pleistocene femora attributed to genus *Homo*, including KNM-ER 803a and 1808, which are craniodentally aligned with *H. erectus sensu lato*. Structural analyses of long bones should not be overlooked as a method for inferring the taxonomic identity of unassociated postcranial remains. Future biomechanical research on hominin femora should include KNM-ER 1592 in a broader phylogenetic and functional comparative context.

ACKNOWLEDGEMENTS

I am grateful to Dr. Emma Mbua, the National Museums of Kenya, and the Kenyan Ministry of Education, Science and Technology for permission to study the fossil specimens housed at the National Museums of Kenya in Nairobi. I

thank Dr. Lindsay J. Foreman for assistance with x-raying the modern human skeletal material. I am deeply thankful to the three anonymous reviewers for their constructive feedback, thoughtful comments, and helpful suggestions that improved this paper. This research was funded by a Graduate Research Thesis Award from the Faculty of Social Sciences at The University of Western Ontario (now Western University).

ENDNOTE

¹The International Commission on Stratigraphy has recently recommended placing the base of the Pleistocene at 2.588 (2.6) Ma, which has been approved by the International Union of Geological Sciences (IUGS) (Gibbard et al. 2010). Throughout this article, however, the base of the Pleistocene is defined as 1.806 Ma (Gradstein et al. 2004) to maintain better consistency with most of the published literature on hominin evolution during the Pleistocene.

REFERENCES

- Antón, S.C., 2003. Natural history of *Homo erectus*. Yearb. Phys. Anthropol. 46, 126–170.
- Berger, L.R., Hawks, J., de Ruiter D.J., Churchill, S.E., Schmid, P., Delezene, L.K., Kivell, T.L., Garvin, H.M., Williams, S.A., DeSilva, J.M., Skinner, M.M., Musiba, C.M., Cameron, N., Holliday, T.W., Harcourt-Smith, W., Ackermann, R.R., Bastir, M., Bogin, B., Bolter, D., Brophy, J., Cofran, Z.D., Congdon, K.A., Deane, A.S., Dembo, M., Drapeau, M., Elliott, M.C., Feuerriegel, E.M., Garcia-Martinez, D., Green, D.J., Gurtov, A., Irish, J.D., Kruger, A., Laird, M.F., Marchi, D., Meyer, M.R., Nalla, S., Negash, E.W., Orr, K.M., Radovic, D., Schroeder, L., Scott, J.E., Throckmorton, A., Tocheri, M.W., VanSickle, C., Walker, C.S., Wei, P., Zipfel, B., 2015. *Homo naledi*, a new species of the genus *Homo* from the Dinaledi Chamber, South Africa. eLife 4, e09560.
- Bertram, J.E.A., Swartz, S.M., 1991. The “law of bone transformation”: A case of crying Wolff? Biol. Rev. 66, 245–273.
- Bleuze, M.M., 2010. Cross-sectional morphology and mechanical loading in Plio-Pleistocene hominins: Implications for locomotion and taxonomy. Ph.D. Dissertation. The University of Western Ontario.
- Bleuze, M., 2012. Proximal femoral diaphyseal cross-sectional geometry in *Orrorin tugenensis*. Homo 63, 153–166.
- Bobe, R., Carvalho, S., 2019. Hominin diversity and high environmental variability in the Okote Member, Koobi Fora Formation, Kenya. J. Hum. Evol. 126, 91–105.
- Bull, S., Spence, M.W., 1988. The Birkette burial. KEWA. Newsletter of the London Chapter Ontario Archaeological Society 6–11.
- Cazenave, M., Braga, J., Oettlé, A., Thackeray, J.F., de Beer, F., Hoffman, J., Endalamaw, M., Redae, B.E., Puymerail, L., Macchiarelli, R., 2017. Inner structural organization of the distal humerus in *Paranthropus* and *Homo*. C. R. Palevol. 16, 521–532.
- Clarke, R.J., 1985. *Australopithecus* and early *Homo* in southern Africa. In: Delson, E. (Ed.), Ancestors: The Hard Evidence. Alan R. Liss, New York, pp. 171–177.
- Currey, J.D., 2003. The many adaptations of bone. J. Biomech. 36, 1487–1495.
- Day, M.H., 1971. Post cranial remains of *Homo erectus* from Bed IV, Olduvai Gorge, Tanzania. Nature 232, 383–387.
- Day, M.H., 1986. Guide to Fossil Man: A Handbook of Human Palaeontology. 4th Edition. The University of Chicago Press, Chicago.
- Day, M.H., Leakey, R.E.F., 1973. New evidence of the genus *Homo* from East Rudolf, Kenya. I. Am. J. Phys. Anthropol. 39, 341–354.
- Day, M.H., Molleson, T.I., 1973. The Trinil femora. Symp. Soc. Stud. Hum. Bol. 11, 127–154.
- Day, M.H., Leakey, R.E.F., 1974. New evidence of the genus *Homo* from East Rudolf, Kenya (III). Am. J. Phys. Anthropol. 41, 367–380.
- Day, M.H., Leakey, R.E.F., Walker, A.C., Wood, B.A., 1975. New hominids from East Rudolf, Kenya, I. Am. J. Phys. Anthropol. 42, 461–476.
- Day, M.H., Leakey, R.E.F., Walker, A.C., Wood, B.A., 1976. New hominids from East Turkana, Kenya. Am. J. Phys. Anthropol. 45, 369–436.
- DeSilva, J., Grabowski, M., 2020. Femur. In: Zipfel, B., Richmond, B.G., Ward, C.V. (Eds.), Hominin Postcranial Remains from Sterkfontein, South Africa, 1936–1995. Oxford University Press, Oxford, pp. 210–229.
- Domínguez-Rodrigo, M., Pickering, T.R., Baquedano, E., Mabulla, A., Mark, D.F., Musiba, C., Bunn, H.T., Uribe-larrea, D., Smith, V., Diez-Martin, F., Pérez-González, A., Sánchez, P., Santonja, M., Barboni, D., Gidna, A., Ashley, G., Yravedra, J., Heaton, J.L., Arriaza, M.C., 2013. First partial skeleton of a 1.34-million-year-old *Paranthropus boisei* from Bed II, Olduvai Gorge, Tanzania. PLoS ONE 3, e80347.
- Feibel, C.S., Brown, F.H., McDougall, I., 1989. Stratigraphic context of fossil hominids from the Omo Group: Northern Turkana Basin, Kenya and Ethiopia. Am. J. Phys. Anthropol. 78, 595–622.
- Feik, S.A., Thomas, C.D.L., Bruns, R., Clement, J.G., 2000. Regional variations in cortical modeling in the femoral mid-shaft: Sex and age differences. Am. J. Phys. Anthropol. 112, 191–205.
- Fornai, C., Krenn, V.A., Mitteroecker, P., Webb, N.M., Haeusler, M., 2021. Sacrum morphology supports taxonomic heterogeneity of “*Australopithecus africanus*” at Sterkfontein Member 4. Commun. Biol. 4, 347.
- Friedl, L., Claxton, A.G., Walker, C.S., Churchill, S.E., Holliday, T.W., Hawks, J., Berger, L.R., DeSilva, J.M., Marchi, D., 2019. Femoral neck and shaft structure in *Homo naledi* from the Dinaledi Chamber (Rising Star System, South Africa). J. Hum. Evol. 133, 61–77.
- Gibbard, P.L., Head, M.J., Walker, M.J.C., the Subcommission on Quaternary Stratigraphy, 2010. Formal ratification of the Quaternary System/Period and the Pleistocene Series/Epoch with a base at 2.58 Ma. J. Quaternary Sci. 25, 96–102.
- Ginter, J.K., 2001. Dealing with unknowns in a non-popu-

- lation: The skeletal analysis of the Odd Fellows series. M.A. Thesis, The University of Western Ontario.
- Ginter, J.K., 2008. Origins of the Odd Fellows skeletal collection: Exploring links to early medical training. Ontario Archaeology No. 85-88/London Chapter OAS Occasional Publication No. 9, 187–203.
- Grabowski, M., Hatala, K.G., Jungers, W.L., Richmond, B.G., 2015. Body mass estimates of hominin fossils and the evolution of human body size. *J. Hum. Evol.* 85, 75–93.
- Gradstein, F.M., Ogg, J.G., Smith, A.G. (Eds.), 2005. *A Geologic Time Scale*. Cambridge University Press, Cambridge. [imprinted 2004].
- Grimaud-Hervé, D., Valentin, F., Sémah, F., Sémah, A., Djubiantono, T., Widiyanto, H., 1994. Le femur humain Kresna 11 comparé à ceux de Trinil. *C. R. Acad. Sci. Paris* 318, 1139–1144.
- Grine, F.E., Jungers, W.L., Tobias, P.V., Pearson, O.M., 1995. Fossil *Homo* femur from Berg Aukas, northern Namibia. *Am. J. Phys. Anthropol.* 97, 151–185.
- Grine, F.E., Delanty, M.M., Wood, B.A., 2013. Variation in mandibular postcanine dental morphology and hominin species representation in Member 4, Sterkfontein, South Africa. In: Reed, K., Fleagle, J., Leakey, R. (Eds.), *The Paleobiology of Australopithecus*. Vertebrate Paleobiology and Paleoanthropology. Springer, Dordrecht, pp. 125–146.
- Haeusler, M., McHenry, H.M., 2004. Body proportions of *Homo habilis* reviewed. *J. Hum. Evol.* 46, 433–465.
- Harmon, E., 2009. Size and shape variation in the proximal femur of *Australopithecus africanus*. *J. Hum. Evol.* 56, 551–559.
- Holliday, T.W., 2002. Body size and postcranial robusticity of European Upper Paleolithic hominins. *J. Hum. Evol.* 43, 513–528.
- Huiskes, R., 1982. On the modeling of long bones in structural analyses. *J. Biomech.* 15, 65–69.
- Jaundrell-Thompson, F., Ashworth, W.J., 1970. *X-ray Physics and Equipment*. 2nd Edition. Blackwell Scientific Publishing, Oxford.
- Johanson, D.C., Lovejoy C.O., Kimbel, W.H., White T.D., Ward, S.C., Bush, M.E., Latimer, B.M., Coppens, Y., 1982. Morphology of the Pliocene partial hominid skeleton (A.L. 288-1) from the Hadar Formation, Ethiopia. *Am. J. Phys. Anthropol.* 57, 403–451.
- Johanson, D.C., Masao, F.T., Eck, G.G., White, T.D., Walter, R.C., Kimbel, W.H., Asfaw, B., Manega, P., Ndessokia, P., Suwa, G., 1987. New partial skeleton of *Homo habilis* from Olduvai Gorge, Tanzania. *Nature* 327, 205–209.
- Kennedy, G.E., 1983a. A morphometric and taxonomic assessment of a hominine femur from the lower member, Koobi Fora, Lake Turkana. *Am. J. Phys. Anthropol.* 61, 429–436.
- Kennedy, G.E., 1983b. Some aspects of femoral morphology in *Homo erectus*. *J. Hum. Evol.* 12, 587–616.
- Lague, M.R., 2014. The pattern of hominin postcranial evolution reconsidered in light of size-related shape variation of the distal humerus. *J. Hum. Evol.* 75, 90–109.
- Lague, M.R., 2015. Taxonomic identification of Lower Pleistocene fossil hominins based on distal humeral diaphyseal cross-sectional shape. *PeerJ* 3, e1084.
- Lague, M.R., Chirchir, H., Green, D.J., Mbua, E., Harris, J.W.K., Braun, D.R., Griffin, N.L., Richmond, B.G., 2019a. Humeral anatomy of the KNM-ER 47000 upper limb skeleton from Ileret, Kenya: Implications for taxonomic identification. *J. Hum. Evol.* 126, 24–38.
- Lague, M.R., Chirchir, H., Green, D.J., Mbua, E., Harris, J.W.K., Braun, D.R., Griffin, N.L., Richmond, B.G., 2019b. Cross-sectional properties of the humeral diaphysis of *Paranthropus boisei*: Implications for upper limb function. *J. Hum. Evol.* 126, 51–70.
- Lanyon, L.E., Rubin, C.T., 1984. Static vs dynamic loads as an influence on bone remodelling. *J. Biomech.* 17, 897–905.
- Leakey, M.G., Leakey, R.E.F. (Eds.), 1978. *The Koobi Fora Research Project, vol. 1: The Fossil Hominids and an Introduction to Their Context 1968–1974*. Clarendon Press, Oxford.
- Leakey, R.E.F., 1971. Further evidence of Lower Pleistocene hominids from East Rudolf, North Kenya. *Nature* 231, 241–245.
- Leakey, R.E.F., 1973a. Evidence for an advanced Plio-Pleistocene hominid from East Rudolf, Kenya. *Nature* 242, 447–450.
- Leakey, R.E.F., 1973b. Further evidence of Lower Pleistocene hominids from East Rudolf, North Kenya, 1972. *Nature* 242, 170–173.
- Leakey, R.E.F., Walker, A.C., 1985. Further hominids from the Plio-Pleistocene of Koobi Fora, Kenya. *Am. J. Phys. Anthropol.* 67, 135–163.
- Leakey, R.E.F., Mungai, J.M., Walker, A.C., 1972. New australopithecines from East Rudolf, Kenya II. *Am. J. Phys. Anthropol.* 36, 235–252.
- Legendre, P., 2018. *lmodel2: Model II regression*. R package version 1.7-3. <https://CRAN.Rproject.org/package=lmodel2>.
- Lepre, C.J., Quinn, R.L., Joordens, J.C.A., Swisher III, C.C., Feibel, C.S., 2007. Plio-Pleistocene facies environments from the KBS Member, Koobi Fora Formation: Implications for climate controls on the development of lake-margin hominin habitats in the northeast Turkana Basin (northwest Kenya). *J. Hum. Evol.* 53, 504–514.
- Lieberman, D.E., Wood, B.A., Pilbeam, D.R., 1996. Homology and early *Homo*: An analysis of the evolutionary relationships of *H. habilis* sensu stricto and *H. rudolfensis*. *J. Hum. Evol.* 30, 97–120.
- Lovejoy, C.O., Heiple, K.G., 1972. Proximal femoral anatomy of *Australopithecus*. *Nature* 235, 175–176.
- Lovejoy, C.O., Meindl, R.S., Ohman, J.C., Heiple, K.G., White, T.D., 2002. The Maka femur and its bearing on the antiquity of human walking: Applying contemporary concepts of morphogenesis to the human fossil record. *Am. J. Phys. Anthropol.* 119, 97–133.
- Marchi, D., Walker, C.S., Wei, P., Holliday, T.W., Churchill, S.E., Berger, L.R., DeSilva, J.M., 2017. The thigh and leg

- of *Homo naledi*. *J. Hum. Evol.* 104, 174–204.
- Marchi, D., Harper, C.M., Chirchir, H., Ruff, C.B., 2019. Relative fibular strength and locomotor behavior in KNM-WT 15000 and OH 35. *J. Hum. Evol.* 131, 48–60.
- Martin, R.B., Burr, D.B., 1989. *Structure, Function and Adaptation of Bone*. Raven Press, New York.
- McHenry, H.M., 1991. Femoral lengths and stature in Pliocene hominids. *Am. J. Phys. Anthropol.* 85, 149–158.
- McHenry, H.M., 1992. Body size and proportions in early hominids. *Am. J. Phys. Anthropol.* 87, 407–431.
- McHenry, H.M., Corruccini, R.S., 1978. The femur in early human evolution. *Am. J. Phys. Anthropol.* 49, 473–488.
- Molto, J.E., Spence, M.W., Fox, W.A., 1986. The Van Oordt site: A case study in salvage osteology. *Can. Rev. Phys. Anthropol.* 5, 49–61.
- Ohman, J.C., Krochta, T.J., Lovejoy, C.O., Mensforth, R.P., Latimer, B., 1997. Cortical bone distribution in the femoral neck of hominoids: Implications for the locomotion of *Australopithecus afarensis*. *Am. J. Phys. Anthropol.* 104, 117–131.
- O'Neill, M.C., Ruff, C.B., 2004. Estimating human long bone cross-sectional geometric properties: A comparison of non-invasive methods. *J. Hum. Evol.* 47, 221–235.
- Parish, J.M., 2000. The Stirrup Court cemetery: An examination of peri-urban health in nineteenth century Ontario. M.A. thesis, The University of Western Ontario.
- Partridge, T.C., Granger, D.E., Caffee, M.W., Clarke, R.J., 2003. Lower Pliocene hominid remains from Sterkfontein. *Science* 300, 607–612.
- Pearson, O.M., Lieberman, D.E., 2004. The aging of Wolff's "Law": Ontogeny and responses to mechanical loading in cortical bone. *Yearb. Phys. Anthropol.* 47, 63–99.
- Pickering, T.R., Heaton, J.L., Clarke, R.J., Stratford, D., Heile, A.J., 2021. Hominin lower limb bones from Sterkfontein Caves, South Africa (1998–2003 excavations). *S. Afr. J. Sci.* 117, 1–10.
- Puymérail, L., Ruff, C.B., Bondioli, L., Widiyanto, H., Trinkaus, E., Macchiarelli, R., 2012. Structural analysis of the Kresna 11 *Homo erectus* femoral shaft (Sangiran, Java). *J. Hum. Evol.* 63, 741–749.
- R Core Team, 2021. R: A language and environment for statistical computing. R Foundation for Statistical Computing, Vienna, Austria. URL <https://www.R-project.org/>.
- Reilly, D.T., Burstein, A.H., 1974. The mechanical properties of cortical bone. *J. Bone Joint Surg.* 56A, 1001–1022.
- Richmond, B.G., Green, D.J., Lague, M.R., Chirchir, H., Behrensmeyer, A.K., Bobe, R., Bamford, M.K., Griffin, N.L., Gunz, P., Mbua, E., Merritt, S.R., Pobiner, B., Kijura, P., Kibunjia, M., Harris, J.W.K., Braun, D.R., 2020. The upper limb of *Paranthropus boisei* from Ileret, Kenya. *J. Hum. Evol.* 141, 102727.
- Rightmire, G. P., 1990 *The Evolution of Homo erectus: Comparative Anatomical Studies of an Extinct Human Species*. Cambridge University Press, Cambridge.
- Rodríguez, L., Carretero, J.M., García-González, R., Arsuaiga, J.L., 2018. Cross-sectional properties of the lower limb bones in the Middle Pleistocene Sima de los Huecos sample (Sierra de Atapuerca, Spain). *J. Hum. Evol.* 117, 1–12.
- Rosenberg, K., Trevathan, W., 1995. Bipedalism and human birth: The obstetrical dilemma revisited. *Evol. Anthropol.* 4, 161–168.
- Ruff, C.B., 1987. Sexual dimorphism in human lower limb bone structure: Relationship to subsistence strategy and sexual division of labor. *J. Hum. Evol.* 16, 391–416.
- Ruff, C.B., 1992. Biomechanical analyses of archaeological human material. In: Saunders, S.R., Katzenberg, M.A. (Eds.), *The Skeletal Biology of Past Peoples*. Alan R. Liss, New York, pp. 41–62.
- Ruff, C.B., 1995. Biomechanics of the hip and birth in early *Homo*. *Am. J. Phys. Anthropol.* 98, 527–574.
- Ruff, C.B., 2000. Body size, body shape, and long bone strength in modern humans. *J. Hum. Evol.* 38, 269–290.
- Ruff, C.B., 2008. Femoral/humeral strength in early African *Homo erectus*. *J. Hum. Evol.* 54, 383–390.
- Ruff, C.B., 2009. Relative limb strength and locomotion in *Homo habilis*. *Am. J. Phys. Anthropol.* 138, 90–100.
- Ruff, C.B., 2019. Biomechanical analyses of archaeological human skeletons. In: Katzenberg, M.A., Grauer, A.L. (Eds.), *Biological Anthropology of the Human Skeleton*. 3rd Edition. John Wiley & Sons, Hoboken, New Jersey, pp. 189–224.
- Ruff, C.B., Hayes, W.C., 1983. Cross-sectional geometry of Pecos Pueblo femora and tibiae—a biomechanical investigation. I: Method and general patterns of variation. *Am. J. Phys. Anthropol.* 60, 383–400.
- Ruff, C.B., Trinkaus, E., Walker, A., Larsen, C.S., 1993. Postcranial robusticity in *Homo*. I: Temporal trends and mechanical interpretation. *Am. J. Phys. Anthropol.* 91, 21–53.
- Ruff, C.B., Walker, A., Trinkaus, E., 1994. Postcranial robusticity in *Homo*. III: Ontogeny. *Am. J. Phys. Anthropol.* 93, 35–54.
- Ruff, C.B., McHenry, H.M., Thackeray, J.F., 1999. Cross-sectional morphology of the SK 82 and 97 proximal femora. *Am. J. Phys. Anthropol.* 109, 509–521.
- Ruff, C.B., Holt, B., Trinkaus, E., 2006. Who's afraid of the big bad Wolff?: "Wolff's Law" and bone functional adaptation. *Am. J. Phys. Anthropol.* 129, 484–498.
- Ruff, C.B., Puymérail, L., Macchiarelli, R., Sipla, J., Ciochon, R.L., 2015. Structure and composition of the Trinil femora: Functional and taxonomic implications. *J. Hum. Evol.* 80, 147–158.
- Ruff, C.B., Burgess, M.L., Ketcham, R.A., Kappelman, J., 2016. Limb bone structural proportions and locomotor behavior in A.L. 288-1 ("Lucy"). *PloS ONE* 11, e0166095.
- Ruff, C.B., Burgess, M., Loring, Squyres, N., Junno, J.A., Trinkaus, E., 2018. Lower limb articular scaling and body mass estimation in Pliocene and Pleistocene hominins. *J. Hum. Evol.* 115, 85–111.
- Ruff, C.B., Higgins, R.W., Carlson, K.J., 2020. Long bone cross-sectional geometry. In: Zipfel, B., Richmond, B.G., Ward, C.V. (Eds.), *Hominin Postcranial Remains from Sterkfontein, South Africa, 1936–1995*. Oxford

- University Press, Oxford, pp. 307–320.
- Shaw, C.N., Stock, J.T., 2011. The influence of body proportions on femoral and tibial midshaft shape in hunter-gatherers. *Am. J. Phys. Anthropol.* 144, 22–29.
- Sládek, V., Berner, M., Galeta, P., Friedl, L., Kudrnová, S., 2010. Technical note: The effect of midshaft location on the error ranges of femoral and tibial cross-sectional parameters. *Am. J. Phys. Anthropol.* 141, 325–332.
- Spence, M.W., 1985. Notes on the Breslau burials. June 11, 1985. Department of Anthropology, The University of Western Ontario, London, Ontario, Canada.
- Spence, M.W., 1994. Mortuary programmes of the early Ontario Iroquoians. *Ont. Archaeol.* 58, 6–20.
- Spence, M.W., Shkrum, M.J., Ariss, A., Regan, J., 1999. Craniocervical injuries in judicial hangings: An anthropologic analysis of six cases. *Am. J. Foren. Med. Path.* 20, 306–322.
- Stock, J.T., 2002. A test of two methods of radiographically deriving long bone cross-sectional geometric properties compared to direct sectioning of the diaphysis. *Int. J. Osteoarchaeol.* 12, 335–342.
- Stock, J.T., Shaw, C.N., 2007. Which measures of diaphyseal robusticity are robust? A comparison of external methods of quantifying the strength of long bone diaphyses to cross-sectional geometric properties. *Am. J. Phys. Anthropol.* 134, 412–423.
- Susman, R.L., de Ruiter, D., Brain, C.K., 2001. Recently identified postcranial remains of *Paranthropus* and early *Homo* from Swartkrans Cave, South Africa. *J. Hum. Evol.* 41, 607–629.
- Trinkaus, E., 1984. Does KNM-ER 1481A establish *Homo erectus* at 2.0 myr BP? *Am. J. Phys. Anthropol.* 64, 137–139.
- Trinkaus, E., 1997. Appendicular robusticity and the paleobiology of modern human emergence. *P. Natl. Acad. Sci. USA* 94, 13367–13373.
- Trinkaus, E., Ruff, C.B., 1999. Diaphyseal cross-sectional geometry of Near Eastern Middle Palaeolithic humans: The femur. *J. Archaeol. Sci.* 26, 409–424.
- Trinkaus, E., Ruff, C.B., 2012. Femoral and tibial diaphyseal cross-sectional geometry in Pleistocene *Homo*. *PaleoAnthropology* 2012, 13–62.
- Trinkaus, E., Ruff, C.B., Conroy, G.C., 1999. The anomalous archaic *Homo* femur from Berg Aukas, Namibia: A biomechanical assessment. *Am. J. Phys. Anthropol.* 110, 379–391.
- Wallace, I.J., Middleton, K.M., Lublinsky, S., Kelly, S.A., Judex, S., Garland Jr., T., Demes, B., 2010. Functional significance of genetic variation underlying limb bone diaphyseal structure. *Am. J. Phys. Anthropol.* 143, 21–30.
- Wallace, I.J., Demes, B., Judex, S., 2017. Ontogenetic and genetic influences on bone's responsiveness to mechanical signals. In: Percival, C.J., Richtsmeier, J.T. (Eds.), *Building Bones: Bone Formation and Development in Anthropology*. Cambridge University Press, Cambridge, pp. 233–253.
- Ward, C.V., Feibel, C.S., Hammond, A.S., Leakey, L.N., Moffett, E.A., Plavcan, J.M., Skinner, M.M., Spoor, F., Leakey, M.G., 2015. Associated ilium and femur from Koobi Fora, Kenya, and postcranial diversity in early *Homo*. *J. Hum. Evol.* 81, 48–67.
- Warton, D.I., Duursma, R.A., Falster, D.S., Taskinen, S., 2012. smatr 3—an R package for estimation and inference about allometric lines. *Methods Ecol. Evol.* 3, 257–259.
- Woo, S.L., Kuei, S.C., Amiel, D., Gomez, M.A., Hayes, W.C., White, F.C., Akeson, W.H., 1981. The effect of prolonged physical training on the properties of long bone: A study of Wolff's Law. *J. Bone Joint Surg. Am.* 63, 780–787.
- Wood, B., Collard, M., 1999. The changing face of genus *Homo*. *Evol. Anthropol.* 8, 195–207.
- Wood, B., Collard, M., 2001. The meaning of *Homo*. *Ludus Vitalis IX*, 63–74.
- Wood, B.A., Leakey, M., 2011. The Omo-Turkana Basin fossil hominins and their contribution to our understanding of human evolution in Africa. *Evol. Anthropol.* 20, 264–292.